Comp 766 - Final Project Report

Stochastic Completion Field with Probabilistic Transition

Shiyan Hu

Biomedical Engineering Department

McGill University

ID No: 260068398

Email: shiyanhu99@yahoo.com

December 22, 2003

Abstract

The report is to present a new simple method of using the probabilistic transition to evaluate the stochastic completion field. It is found that by quantizing the imaging plane according to the actual line-up of the image pixels, the stochastic completion field with random walks can be well characterized by the transition probabilities. Those transition probabilities can be calculated from either the original Gaussian probability density function for the random walk or some intuitive formulae directly related to the energy of a continuous curve. With the probabilistic transition, the stability can be assured by selecting a good decay factor and the steady state can be calculated especially when the size of the image is small. For large size image, the local concurrent update based on the transition probabilities has to be carried out. The resulting performance will be more accurate than that estimated from the Monte Carlo simulation of many random walks and the complexity is much less. Several results are shown to demonstrate the use of the probabilistic transition.

Table of Contents

1 INTRODUCTION 1

2 PRELIMINARIES OF STOCHASTIC COMPLETION FIELD 3

2.1 RANDOM WALK FOR DISTRIBUTION CHARACTERIZATION 3
2.2 STOCHASTIC COMPLETION FIELDS 4

3 STOCHASTIC COMPLETION FIELDS WITH PROBABILISTIC TRANSITION 5

3.1 LINE-UP OF IMAGE PIXELS 5
3.2 TRANSITION PROBABILITIES OF RANDOM WALK 6
3.2.1 Choice of step-size 6
3.2.2 Determination of transition probability 6
3.2.2.1 Eight orientations 6
3.2.2.2 Sixteen orientations 8
3.3 STOCHASTIC COMPLETION FIELD WITH PROBABILISTIC TRANSITION 8
3.4 STABILITY AND STEADY STATE OF STOCHASTIC COMPLETION FIELDS 9

4 GENERAL TRANSITION PROBABILITIES FOR STOCHASTIC COMPLETION FIELDS 11

4.1 ENERGY OF A CONTINUOUS CURVE 11
4.2 GENERAL CALCULATION OF TRANSITION PROBABILITY 11

5 ILLUSTRATIVE RESULTS 13

5.1 VALIDATION OF PROBABILISTIC TRANSITION 13
5.2 EFFECT OF VARIANCE σ^2 14
5.3 EFFECT OF DECAY CONSTANT 15
5.4 EXAMPLES OF COMPLETION FIELDS 16

6 CONCLUSIONS AND FUTURE WORK 21

7 ACKNOWLEDGMENTS 22

8 REFERENCES 23

Table of Figures

Figure 1 Line-up of the image pixels.....5
Figure 2 Eight pixels and eight orientations for transition probability calculation.....6
Figure 3 Integration interval for transition probabilities.....7
Figure 4 Eight pixels and sixteen orientations for transition probability calculation. 8
Figure 5 $P(u,v,\phi)$ in a 16×16 image with initial state (2,8,0) and r=1, τ =10, m=8, N=20, σ^2 =0.25.....14
Figure 6 $P(u,v,\phi)$ in a 16×16 image with initial state (2,8,0) and r=1, τ =10, m=8, N=20, σ^2 =0.1 15
Figure 7 $P(u,v,\phi)$ in a 16×16 image with initial state (2,8,0) and r=1, τ =1, N=20, σ^2 =0.25 15
Figure 8 Stochastic source field in a 32×32 image with r=1.31, τ =10, m=16, N=32, σ^2 =0.01.....16
Figure 9 Stochastic sink field in a 32×32 image with r=1.31, τ =10, m=16, N=32, σ^2 =0.01. 17
Figure 10 Stochastic completion field in a 32×32 image with r=1.31, τ =10, m=16, N=32, σ^2 =0.01. 17
Figure 11 Stochastic completion field with orientation for source/sink pair: (2,23,2)/(46,23,12), in a 48×48 image with r=1.31, τ =10, m=16, N=48, σ^2 =0.02. 19
Figure 12 Stochastic completion field with intensity for source/sink pair: (2,23,2), (46,23,12), in a 48×48 image with r=1.31, τ =10, m=16, N=48, σ^2 =0.02. 19
Figure 13 Stochastic completion field with orientation for source/sink pair: (2,23,2)/(46,23,2), in a 48×48 image with r=1.31, τ =10, m=16, N=48, σ^2 =0.05. 20
Figure 14 Stochastic completion field with intensity for source/sink pair: (2,23,2)/(46,23,12), in a 48×48 image with r=1.31, τ =10, m=16, N=48, σ^2 =0.05. 20

Table of Tables

Table 1 Relative probabilities of each pixel in a 3×3 image with source in state (2,2,0).....13
Table 2 Relative probabilities of each pixel in a 4×4 image with source in state (2,2,0).....14

1 Introduction

The completion of illusory contour and salience is to determine the shape or compute the relative likelihood from a family of curves that potentially connect (or complete) a set of boundary fragments. Such completion analysis is very useful in the computer vision that has an objective of discovering from images what is and where in the world and has the need of recognizing, from the visible surfaces, shapes and structures that form an image [1]. As many problems in vision, such figural completion is ill-posed due to the fact that the precise shape of an object's boundary might be hidden from viewer by another object and cannot be known precisely to the visual system, what the visual system can do the best is a guess established on the maximum likelihood estimate. A general formula used to measure the likelihood is related to the distance $\int ds$ for arc length *s*, and the bending energy $\int \kappa^2(s)ds$ for curvature $\kappa(s)$. The likelihood function can be written as $E = \alpha \int ds + \beta \int \kappa^2(s)ds$ with α and β as weighting coefficients to weight the distance and bending energy in the overall likelihood estimate. The completion analysis is to find an illusory contour that minimizes the likelihood function *E*.

Over the years, much work has been devoted to the formulation of the computational models of perceptual completion and illusory contours [2-6]. In particular, Ullman proposed to join two contour fragments based on a "two-circular arcs" construction with each circular arc being tangent to its sponsoring contour at one end and to the other arc at the point of intersection [2]. Such "two-circular arcs" assumption is to mimic the two eyes structure in the human visual system and this is probably the earliest theory for illusory contour shape. The final shape can be modeled from the circular pair that minimizes the total bending energy. In [3], a bank of kernel filters with various orientations were used to convolve the image in the first stage followed by a second non-linear synthesis processing stage to combine the outputs from various kernel filters. Unfortunately, the size of the kernel filter is large and it creates a burden of computation complexity. Also, the synthesis processing is difficult as the illusory contours can be suggested from many different forms of stimulus. With a similar two stage structure to that in [3], Parent and Zucker [4] presented a novel approach to curve inference from the tangent and curvature information with the first stage for trace inference and the second stage for curve synthesis. Their approach distinguished itself from others in two aspects: a local-to-global step to determine the trace points without knowing the priori knowledge, and a function for curvature variation for which the minimization is using standard relaxation labeling techniques. This approach can be used to model illusory contour shape as discussed in [5], which showed the use of tangent and curvature information in locating the valleys, i.e., mode or ridge lines. Another method to represent the global image structure from local tangent measurements can be found in [6], where the local summation of a set of global voting patterns was proposed. The voting pattern was a vector-field and was used to present the orientations that were co-circular to the tangent measurements. The resulting vector-field was deterministic and it might be difficult to model the priori distribution of the completion shapes [7].

In recent years, Williams et al has presented a concept of stochastic completion field, where the random walk wandering over the lattice with orientations was used to model the prior probability distribution of boundary completion shape. The model appears to be simple and is free of any numerical relaxation or other explicit minimization. In [7], a neural model was used and Monte Carlo simulation was carried out to estimate the transition probabilities. A further local parallel computation [9] was proposed to employ the Fokker-Planck equation to simplify the integration in the stochastic process. The resulting complexity is $O(n^3 m)$ for an $n \times n$ image with m discrete orientations as compared to $O(n^4 m^2)$ in approaches of convolving large-kernel filters. More recently, an analytical solution for such stochastic completion fields has been addressed in [8] to characterize the probability distribution of boundary-completion shape and illustrate explicitly the relationship between velocity, diffusivity, and decay. The analytical approach involved one-dimensional integration in computing the fraction, and the integration could be carried out numerically. However, all the above approaches did not consider the actual line-up of the image pixels and they had to use

the probability density function to characterize the distribution, resulting in the integration-involved formula in computing the stochastic completion field. Sometimes, an approximation was used to estimate the integral as in [9]. Therefore, it is of interest to study a method that can reduce the computational complexity and can provide a base for analytical solution as well.

In this report, we propose to characterize the stochastic completion filed with the probabilistic transition by using the transition probabilities computed from the actual line-up of the image pixels. Specifically, we consider the actual line-up of the image pixels that can be thought of the quantization of the image plane. As such, the wander of the random walk can be limited to a fixed number of positions that are determined by the step size of the random walk. The number of orientations can be arbitrary, denoted by m for m orientations. The transition probability to each position can be pre-calculated from either the original Gaussian distribution or a general cost function related to the relative likelihood function as previously mentioned. As the transition probabilities are the same for all the pixels, the analytical solution of the stochastic field can be carried out straightforwardly from the matrix inverse. It is found that for small size image, the analytical solution can be obtained easily and the results are shown in a good agreement with those from the Monte Carlo random walk simulation. For large size image, the analytical solution is difficult to compute due to the huge size of the transition probability matrix. Therefore, the idea of the local parallel computation [9] is adopted. Each time, all the pixels in the image can update in a local concurrent fashion their probabilities (or likelihood). However, as a point of differing our approach from that in [9], our approach needs no integration and no approximation. Consequently, for each update, each pixel needs to compute m transitions. The overall computational complexity is $O(n^2 m t)$ for an $n \times n$ image with m discrete orientations and t update steps, which is inline with that of the local parallel computation [9]. The stability of this probabilistic transition is discussed and it is shown that as long as the decay factor is properly selected, the convergence of the transition can be achieved. Several illustration results are presented to demonstrate the usefulness of this probabilistic transition.

The report is organized as follows. Some preliminaries of the stochastic completion field are reviewed in Section 2. Section 3 examines the quantization of the stochastic completion field from the actual line-up of the image pixels and proposes a probabilistic transition concept. The stability and steady state of the completion field with probabilistic transition are also addressed. Section 4 discusses a general intuitive method related to bending energy and distance. The simulation results are presented in Section 5. Finally, Section 6 concludes the report and provides the discussion on the possible future work.

2 Preliminaries of Stochastic Completion Field

The stochastic completion field was inspired by the thought that a random walk wandering with orientations in an image plane can be used to model the probability distribution of boundary completion [7, 10]. In this section, we will give a brief review on random walk and the stochastic completion field for illusory contour shape and salience.

2.1 Random Walk for distribution characterization

The completion field in the shape analysis is an important step in the computer vision system, which was originated from mimicking the human vision system. Therefore, to understand better the completion field, it is of interest to begin with the biological findings in the human vision system.

Biology study [11, 12] showed that the retinal ganglion cells and the cells of the lateral geniculate in the human vision system were with concentric, center-surround receptive fields, and they were spotlight sensitive and would narrowly tune to stimuli of specific position and orientation. Those cells can be found in lower part (V1) of one layer in prime visual cortex and they are responsible as suggested in [13] of mapping under the guidance of maximizing locality a $R^2 \times S^1$ space with positions and orientations onto a two-dimensional surface R^2 in the cortex. Because of the dimension reduction in the mapping, the shape of an object's boundary might be hidden behind another object and cannot be known precisely to the visual system. The completion field tries to solve this problem.

Given the fact that the visual system can view the surface to obtain a set of boundary fragments, the best it can do to reconstruct the shape is to guess the shape to have a completion of an illusory contour in the light of maximum likelihood estimate: given the prior probability distribution of the completion shapes, choose a most probable contour. In [7], instead of computing the maximum likelihood completion shape, a simple concept of computing local image plane statistics of the distribution of possible completion shapes was proposed. This agrees well with the biological finding on the local computation in the V1 cortex and is psychophysically meaningful.

To model the distribution of completion shapes, Markov process is used and simulation of random walks wandering in a stochastic motion can be carried out. A random walk is normally defined with two elements: motion equation and decay constant. The motion equation determines the change in a particle's position. For a random walk at position (*x,y*) with orientation θ, or equivalently in state (x,y,θ), its motion (differential) equation is

$$\dot{x} = r\cos\theta, \qquad \dot{y} = r\sin\theta, \qquad \dot{\theta} = \hat{\kappa}(0,\sigma^2;t) \tag{1}$$

where $\dot{x}$ and $\dot{y}$ denote the change in position with step size *r*, $\dot{\theta}$ is the change in orientation related to curvature and $\hat{\kappa}(0,\sigma^2;t)$ is a normally (Gaussian) distributed random variable with zero mean and variance σ^2.

The choice of the Gaussian distribution for orientation change also has its biological support. Specifically, in the cortex, the cells with similar complexity are grouped in layers and the neighboring cells have the close and actually overlapped receptive fields, the size of which varies and is related to the eccentricity: the distance of a cell's receptive field from the center of gaze [12]. This suggests that the retina analyzes the visual scene in detail in the central part but in a blur manner in the periphery. The Gaussian distribution is very much inline with those findings. Please note that in the above equation (1), the step size *r* is introduced to the change of positions. This is different from the equation in [7], where *r* is set to 1 all the time. Later, we will see that such additional parameter *r* can control the transition probabilities.

The decay constant in the random walk describes a particle's average lifetime and it assumes that a certain fraction of particles will decay per unit time and thus the longer paths are less likely.

2.2 Stochastic Completion Fields

As pointed out by Williams [7], the activity of the cells in the V1 can be characterized by a probability density function (PDF) defined over $R^2 \times S^1$ and a network of interconnections in terms of transition probabilities among them from $R^2 \times S^1$ plane to $R^2 \times S^1$ plane. The transition probability that a random walk of length *t* can be represented by the Green's function, i.e., $G(u,v,\phi,x,y,\theta;t)$, which denotes the probability that a random walk of length *t* will begin in state (x,y,θ) and end in state (u,v,ϕ). The PDF of a particle in state (u,v,ϕ) at time instant *t*, denoted by $p(u,v,\phi;t)$ can be written as

$$p(u,v,\phi;t) = \int_{-\infty}^{\infty} dx \int_{-\infty}^{\infty} dy \int_{-\pi}^{\pi} d\theta \; G(u,v,\phi,x,y,\theta;t)\, p(x,y,\theta;0)\, e^{-t/\tau} \qquad (2)$$

where $p(x,y,\theta;0)$ is the PDF of a particle in the initial state (x,y,θ) at time instant 0, and $e^{-t/\tau}$ is the result of the decay constant that is assumed to be $(1-e^{-1/\tau})$ per unit time.

The $G(u,v,\phi,x,y,\theta;t)$ function is translated or rotated from the one that assumes the random walks to start in the state (0,0,0), i.e., to transform the co-ordinate system to (x,y,θ) from (0,0,0). We have

$$G(u,v,\phi,x,y,\theta;t) = G(u',v',\phi',0,0,0;t)$$

where $u' = (u-x)\cos\theta + (v-y)\sin\theta$ and $v' = -(u-x)\sin\theta + (v-y)\cos\theta$, and $\phi' = \phi - \theta$.

The stochastic source filed is the fraction of paths beginning at a source state and passing through (u,v,ϕ), which can be given by [7]

$$p'(u,v,\phi) = \int_{0}^{\infty} dt \; p(u,v,\phi;t) = \int_{-\infty}^{\infty} dx \int_{-\infty}^{\infty} dy \int_{-\pi}^{\pi} d\theta \; G'(u',v',\phi')\, p(x,y,\theta;0)$$

where $G'(u',v',\phi') = \int_{0}^{\infty} dt \; G(u,v,\phi;t)\cdot e^{-t/\tau}$.

In a similar manner, a stochastic sink field, denoted by $q'(u,v,\phi)$, can be defined to represent the fraction of paths beginning at state (u,v,ϕ) and finally reaching a sink state. It is found that the stochastic sink field can be regarded as a stochastic source field with 180° degree orientation rotation. For this reason, we did not repeat the expression formulae here.

Finally, the stochastic completion field, $C(u,v,\phi)$, which represents the relative likelihood of a particle leaving a source state, passing through (u,v,ϕ), and entering a sink state, is the product of the source and sink fields [7], i.e.,

$$C(u,v,\phi) = p'(u,v,\phi)\cdot \; q'(u,v,\phi)$$

To implement the above computation, a straightforward method based on the Monte Carlo simulation can be carried out as in [7]. However, the accuracy of the Monte Carlo simulation seems not good enough as in order to obtain an accurate number, it needs a huge number of random walks which is unfortunately limited by the computer memory. On the other hand, the analytic solution of the above stochastic completion fields can be found in [8], where the authors derived the expression to characterize the probability distribution of boundary completion shape and to show the relationship between velocity, diffusivity, and decay. A simple analytical approach based on local parallel computation can be used [9]. In the local parallel computation, the integration in the stochastic completion fields can be simplified by adopting the Fokker-Planck equation and approximating the integral by the summation.

From the above description of the stochastic completion field, we can see that the computational burden is from the integration. As to be pointed out in the next section, if we take into account the actual line-up of the image pixels so as to break down the integration naturally to the summation, the overall computation for the stochastic completion fields can be greatly simplified.

3 Stochastic Completion Fields with Probabilistic Transition

In this section, we will first check the line-up of the image pixels and its effect on the stochastic completion fields. Then, we will compute the transition probabilities based on the actual line-up of the image pixels. Following that, the stability and the steady state of the completion filed are addressed. Finally, for large size image, where the analytical solution might be difficult, the update in a local concurrent fashion can be conducted.

3.1 Line-up of image pixels

The stochastic completion fields discussed in the literature [7-9] did not consider the actual line-up of the image pixels, while in the experiments the quantization was assumed nevertheless. In the following, we attempt to use the knowledge of the line-up in image pixels in order to simplify in the first place the analysis of the stochastic completion field.

We make the following assumptions.

A. Assumption A: Without loss of generality, the image is assumed to start from the origin (0,0) and the size of each square pixel to be 1 (Note that our probabilistic approach to be developed is not limited to the square pixel and it can be extended to the rectangular pixel with minor modifications. Here, for the sake of simplicity in presentation, we consider a square pixel).
B. Assumption B: The position of the random walk will be quantized to the point in the middle of the nearest square pixel. This assumption is reasonable due to the fact that the pixel is the smallest element in the image and there is no need to distinguish the fractional position within one pixel. When a pixel is turned on, the whole pixel is in bright.

As an illustration, the actual line-up of the image pixels for an 8×6 image can be shown in Figure 1.

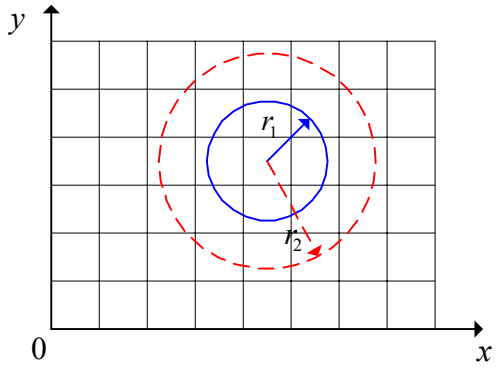

Figure 1 Line-up of the image pixels

In Figure 1, we consider a random walk begins in the position (x,y)=(4.5, 3.5) and it will be in stochastic motion with either step-size r_1 or r_2 according to the differential update equation (1). After its position change, its actual position will be quantized to the center point of the nearest pixel. As we can see, because of the quantization, the number of the possible next-step pixels that the random walk can move into is deterministic for each motion and it is solely dependent on the step-size r. As illustrated in the figure, for step-size r_1, the number is 8, while for r_2 the number is 16.

Although the number of the possible next-step pixels actually determines the number of orientations of the random walk (m), and from the view of the actual line-up of the image pixels, the number of possible next-step positions and that of the orientations are deterministic, in practice, we still allow the number of orientations be more than eight even for the case of eight possible neighboring pixels. The reason for such arrangement is that the orientation at each pixel is related to the curvature that needs a curve with more than

two pixels to determine. Also setting the number of orientations to be more that eight even for the case with step-size r_1 in Figure 1, the completion shape will be more smoothly.

With the information of the next step pixels and the number of orientations, the transition probability from the current pixel to its next-step pixel can be evaluated and the resulting stochastic completion field can be greatly simplified.

3.2 Transition probabilities of random walk

As the number of possible next-step pixels that a random walk can move into is deterministic, we may use the transition probability to characterize the behavior of the random walk. We need to discuss the choice of the step-size first.

3.2.1 Choice of step-size

The choice of the step-size might affect the number of possible next-step pixels as previously illustrated in Figure 1. Due to the fact that the larger step-size might jump over some neighboring pixels and the pixel is the smallest unit in the image, it is of great interest to choose the small step-size to achieve a fine-tuning in the completion field. For this reason, we limit our discussion on the step-size of r_1 as shown in Figure 1 so that eight neighboring pixels are taken into consideration. One might argue that this limitation will also limit the possibilities that the random walk can wander. Our explanation for this is from the fact that by using the smallest element such as pixel, any curve in the image can be approximated. It appears that there is no need to consider more than eight pixels.

Now, we consider a pixel that accommodates one random walk and its eight neighboring pixels as shown in Figure 2. Again, the step-size for the stochastic motion can be any value in the range of (0.5, 1.5]. The choice of the step-size must be larger than 0.5 is quite simple as the random walk with step-size less than 0.5 will step in its current pixel forever according to the assumption (B) for quantization in Section 3.1. The step-size must be less than 1.5 to keep the transition among its eight neighboring pixels.

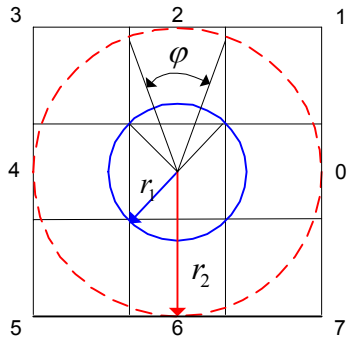

Figure 2 Eight pixels and eight orientations for transition probability calculation.

3.2.2 Determination of transition probability

3.2.2.1 Eight orientations

We discuss eight orientations first. From Figure 2, it can be readily seen that the number of orientations is eight with indices *i*=0,1,…,7 for $i \cdot 2\pi/8$ radians, or equivalently for eight pixels *i*=0,1,2…,7 as labeled in the figure. As the stochastic motion is based on $\dot{\theta}$ that is a normally distributed random variable *w*, the transition probability for a pixel along the orientation *i* is related to the original orientation and the step-size *r*. As an illustration, we assume the original orientation of the random walk is index 0 and the step-size *r* for the stochastic motion (such as r_1 or r_2 in Figure 2). The angle corresponding to the one within the pixel *i* is given by

$$\varphi_i = \begin{cases} 2\sin^{-1}(1/2r) & i = 0,2,4,6 \\ \pi/2 - \varphi_0 & i = 1,3,5,7 \end{cases} \tag{3}$$

The transition probability from the current (source) pixel with orientation 0 to the destination pixel 0 with orientation 0 is equal to the probability that the random variable w falls into the interval ($-\varphi_0/2+2k\pi$, $\varphi_0/2+2k\pi$), where k is an integer number from -∞ to ∞ and $2k\pi$ is introduced as w can take values from -∞ to ∞ while the angle is repeated every 2π. In other words, the transition probability is the integration of a folded Gaussian PDF within the corresponding angle interval. For the destination pixel 1, the interval is ($\varphi_0/2+2k\pi$, $\varphi_0/2+\varphi_1+2k\pi$). For the destination pixel 2, the interval is ($\varphi_0/2+\varphi_1+2k\pi$, $\varphi_0/2+\varphi_1+\varphi_2+2k\pi$), and so on so forth.

Following the above illustration, we can see that if the source pixel is with orientation 1, the integration interval will be a little bit different. A general description of the integration interval can be found in Figure 3, where the Gaussian PDF and the integration intervals for interval indices 0,1,…,7 are shown for one 2π period. The interval corresponding to the peak would be for the destination orientation along with the source orientation. For this reason, in the figure, we use φ_o' and φ_1' to distinguish the even and odd intervals. If the source orientation index is an even number, we set $\varphi_o' = \varphi_o$ and $\varphi_1' = \varphi_1$. Otherwise, we set $\varphi_o' = \varphi_1$ and $\varphi_1' = \varphi_0$. Note that φ_0 and φ_1 are computed from equation (3).

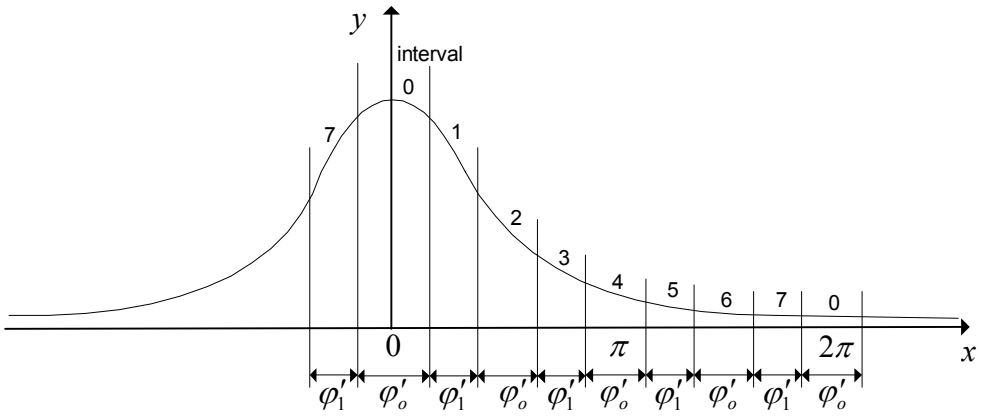

Figure 3 Integration interval for transition probabilities

By using the integration intervals in Figure 3, the transition probability for a random walk with orientation j moving to a pixel with orientation i is given by

$P_T(i \mid j) =$ Integration of intervals with index (i-j) mod 8

$$= \sum_{k=-\infty}^{\infty} \left[\frac{1}{2} erfc\left(\frac{a_{(i-j)\bmod 8} + 2k\pi}{\sqrt{2\sigma^2}} \right) - \frac{1}{2} erfc\left(\frac{b_{(i-j)\bmod 8} + 2k\pi}{\sqrt{2\sigma^2}} \right) \right] \tag{4}$$

where *(i-j) mod 8* is the interval index taken from the set {0,1,…,7}. For even or odd j, φ_o' and φ_1' will be different as explained previously. $a_{(i-j)\bmod 8}$ and $b_{(i-j)\bmod 8}$ are the lower and upper bounds of the corresponding interval. $erfc(x) = \frac{2}{\sqrt{\pi}} \int_x^{\infty} e^{-t^2} dt$ is the error function to indicate the integration of the Gaussian distribution from x to infinity. In our evaluation, we will choose a large enough number (such as 1000) to replace the infinity and then we will check $\sum_{i=0}^{7} P_T(i \mid j)$ which should be equal to 1 for arbitrary j.

It is noteworthy to mention that the reason we have to distinguish the even or odd source orientation is due to the fact that φ_i from equation (3) could be different for even or odd *i*. This might be not desired in the stochastic completion fields as all the orientations shall be made with equal probability. The equal probability over all the orientations can be achieved by setting $2\sin^{-1}(1/2r) = 2\pi/8$, resulting in the best choice for *r,*

$$r = 1/2\sin(\pi/8) = 1.3066 \quad (5)$$

From the above, we can see that by using the actual line-up of the image pixels, the behavior of the random walk can be well described by its transition probabilities. This agrees with the characteristic of the random walk as it is a Markov process as mentioned in [7].

3.2.2.2 Sixteen orientations

In the previous Section 3.2.2.1, our discussion was limited to eight orientations. Actually, we need to discuss more than eight orientations to have a better (and more general) consideration of the curvature. As an example, we consider sixteen orientations in the following. Note that the number of neighboring pixels considered for the next step position is still eight.

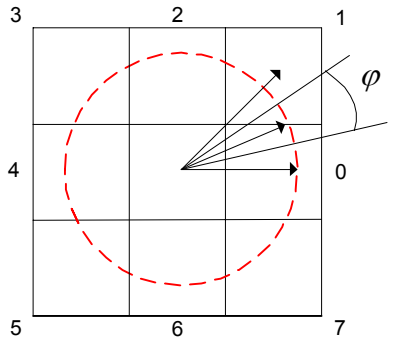

Figure 4 Eight pixels and sixteen orientations for transition probability calculation.

In Figure 4, eight pixels and sixteen orientations for transition probability calculation is plotted. The sixteen orientations are with indices *i*=0,1,…,15 for $i \cdot 2\pi/16$ radians. Evidently, for orientations with even indices, their next-step pixels are known for sure. For orientations with odd indices, their next-step pixels have two possibilities as shown in the figure for the orientation index *i*=1 with angle φ whose next-step could be either pixel 0 or pixel 1. As a result, the transition probability can be calculated in the same way as in Equation (4) (Here, again we can consider that the step-size is chosen to be the one in Equation (5) for the fairness towards all orientations). The only difference is that for the odd indices of orientations, it will split its corresponding transition probabilities into two for two next-step pixels.

The above discussion for sixteen orientations can be extended to the case with even more orientations. Here, due to the limitation of the paper length, we will not discuss further.

3.3 Stochastic completion field with probabilistic transition

From the discussion in the previous section, we know that the transition probabilities can well characterize the random walk. Actually, those transition probabilities are the same for any pixel in an image. If the pixel is at the edge, some transition probabilities are corresponding to the transition from the current pixel to the pixels outside of the $n \times n$ image, and they can be ignored if we assume that the random walk that moves outside the $n \times n$ image is considered to disappear (decay). Because of the quantized orientations, deterministic next-step pixels, and given $n \times n$ size image, there is no need to simulate the random walk for the continuous probability distribution estimate. Rather, one can directly compute the probability distribution as in the discrete case. Further, because we choose $r < 1.5$, only the neighboring pixels are to be considered. As a result, equation (2) becomes a probability (not PDF anymore) $P(u, v, \phi; t)$ that a random walk in state

(u,v,ϕ) at time instant *t* and it can be computed from the neighboring state at time instant *t-1* and the transition probabilities, i.e.,

$$P(u,v,\phi;t) = \sum_{neighboring(x,y)} \sum_{\theta=0}^{m} P_T(\phi \mid \theta)\, P(x,y,\theta;t-1)\; e^{-1/\tau} \tag{6}$$

where ϕ and θ are considered to be one of m orientations, and $e^{-1/\tau}$ is from the decay constant of the random walk.

The probability distribution for source field can be computed by summarizing $P(u,v,\phi;t)$, i.e.,

$$P(u,v,\phi) = \sum_{t=0}^{\infty} P(u,v,\phi;t) \tag{7}$$

In computer simulation, we may just choose a large enough $t=N$ as the stop point of update.

The update equations (6)-(7) are for the stochastic source field. The update equation for the stochastic sink field $Q(u,v,\phi)$ can be carried out in the same way except that the orientation has to be rotated by π radians.

$$Q(u,v,\phi) = P(u,v,\phi+\pi) \tag{8}$$

Finally, the completion field can be computed as the produce of the stochastic source and sink fields similarly as in the continuous case [7].

$$C(u,v,\phi) = P(u,v,\phi)\cdot Q(u,v,\phi) \tag{9}$$

We once wonder whether or not the operator "+" instead of "." can be used for the computation of $C(u,v,\phi)$ as $P(u,v,\phi)$ and $Q(u,v,\phi)$ are for the intensities. However, the operator "." has the support from the probability theorem for the probability of the joint events, and the resulting completion shape is much better than that with the operator "+".

It is noteworthy to mention that the update equation (6) for the probability computation can be considered as a local concurrent update. However, this equation distinguishes itself from the one in [9] in the fact that the equation (6) is the direct result from the line-up or quantization of the image pixels and free from any approximation. Compared with the Monte Carlo simulation for stochastic completion fields, our approach can give more accurate results and it requires much less memory.

3.4 Stability and steady state of stochastic completion fields

By using the above local probabilistic transition to characterize the behavior of the random walks, the stability and steady state of the stochastic completion fields can be easily computed. Specifically, we may re-write the equation (6) in a matrix notation

$$V_P(u,v;t+1) = \sum_{i_1=-1}^{1} \sum_{i_2=-1}^{1} \rho\, M_{P_T}^{(i_1,i_2)}(u,v)\, V_P^{(i_1,i_2)}(u,v;t) \tag{10}$$

where $V_P(u,v;t) = \left[P(u,v,\phi;t) \mid \phi = 0,1,2,...,m\right]^T$ is the column vector for probabilities $P(u,v,\phi;t)$ with size $m\times 1$ for all m possible orientations at time t. $V_P^{(i_1,i_2)}(u,v;t) = V_P(u+i_1,v+i_2;t)$ is the probability vector at the neighboring pixel of the pixel (u,v). $M_{P_T}^{(i_1,i_2)}(u,v)$ is the matrix for transition probabilities from the neighboring pixel $(u+i_1,v+i_2)$ from the orientation θ=0,1,2,…m, to ϕ= 0, 1, 2, …., m. In our case, m=8 or 16. In equation (10), the parameter $\rho = e^{-1/\tau}$ resulted from the decay constant of the random walks.

For all the possible pixels (u,v) in an $n\times n$ image, we can line up all the vectors $V_P(u,v;t)$ into a super vector and re-write (10) into the form of

$$\mathbf{V}_P(t+1) = \rho\; \mathbf{M}_T \mathbf{V}_P(t) \tag{11}$$

where $\mathbf{V}_P(t)$ is the vector that consists of all $V_P(u,v;t)$ or equivalently all possible $P(u,v,\phi;t)$ in an $n \times n$ image. The size of $\mathbf{V}_P(t)$ is $n \times n \times m$. $\mathbf{M}_T$ is a transition matrix consisting of all $m \times m$ $M_{P_T}^{(i_1,i_2)}(u,v)$ matrices and with the size $(n \times n \times m) \times (n \times n \times m)$.

Using (7), the final probability for source field after *N*-step update can be given by

$$\mathbf{V}_P = \sum_{t=0}^{N} \mathbf{V}_P(t) = \sum_{t=0}^{N} [\rho\ \mathbf{M}_T]^t \mathbf{V}_P(0) = (\mathbf{I} - \rho \mathbf{M}_T)^{-1} \left(\mathbf{I} - (\rho \mathbf{M}_T)^{N+1}\right) \mathbf{V}_P(0) \qquad (12)$$

where $\mathbf{V}_P(0)$ is the initial probability at time 0.

For the stability of the source field, the following conditions have to be satisfied.

1. The matrix $(\rho \mathbf{M}_T)^{N+1}$ must converge to zero as *N* approaches infinity. Let $\{\lambda_i\}$ denote the eigenvalues of the matrix $\mathbf{M}_T$. This condition requires that $|\rho \lambda_i| < 1$ for all the eigenvalues.
2. The matrix $(\mathbf{I} - \rho \mathbf{M}_T)$ is invertible. In other words, its eigenvalue must be non-zero. Given the eigenvalues $\{\lambda_i\}$ of the matrix $\mathbf{M}_T$, the eigenvalues of the matrix $(\mathbf{I} - \rho \mathbf{M}_T)$ can be found to be $1 - \rho \lambda_i$. As $|\rho \lambda_i| < 1$ from the first condition, $1 - \rho \lambda_i \neq 0$ holds. Therefore, as long as the condition 1 holds, the condition 2 will be satisfied.

The final steady state for the source field is given by

$$\mathbf{V}_P = (\mathbf{I} - \rho \mathbf{M}_T)^{-1} \mathbf{V}_P(0) \qquad (11)$$

It suggests that the steady state probability can be calculated directly from the overall transition matrix. Unfortunately, this is useful only when the image size is small. For large image size, it is difficult to compute the inverse of the huge matrix, and hence the local update equation in (6) has to be used.

From the above two conditions, we can see that the decay factor ρ plays an important role in the stability control of the stochastic field. Small ρ (implies small τ) can always assure the stability of the stochastic field but it might affect the quality of the illusory contour as the average lifetime of the random walk is limited. In practical evaluation, it might be useful to just perform a large enough *N* steps (for example *N*=*n*, the image size as in [9]) for the stochastic completion field.

As a summary, the stochastic completion fields with probabilistic transition is established from the actual line-up of the image pixels and the quantization assumption. The transition probabilities are found related to the Gaussian PDF and the resulting update equation can be carried locally. In next section, we will generalize the result to use directly the minimum bending energy and minimum distance criteria.

4 General Transition Probabilities for Stochastic Completion Fields

The previous section, the transition probabilities for the stochastic completion fields were found related to the Gaussian probability density function. In this section, the computation for the transition probabilities will be generalized to have a relation directly from the bending energy and minimum distance.

4.1 Energy of a continuous curve

In the completion fields, the diffusion process is closely related to the curves of least energy [7]. A general formula for the energy of the continuous curve can be written as

$$E=\alpha\int ds+\beta\int \kappa^2(s)\,ds \qquad (12)$$

where α and β are weighting coefficients to weight the distance and bending energy in the overall energy.

For the distance factor, we considered in the previous section that the random walk could have the same step-size over all directions and therefore there was no need to consider the cost of the distance. Please note that from the line-up of the image pixels in Figure 1, one might argue (as we originally thought) that even in the case with the constant step, the distances from the central point of the current pixel to the central points of its eight neighbors are different (see Figure 1). We finally declined this argument as otherwise the cost of distance would render the computation in favor of the orientations parallel to *x* or *y* axes. A second question one might ask is: when will the equation in (12) be used? From the equation (1), we know that the random walk might take the step-size *r* in its stochastic motion. If the random walk is allowed to pace with different step-sizes towards different orientations, the contribution of the distance must be taken into account.

For the curvature calculation, the previous section used the one approximated by the Gaussian PDF. By tuning the variance of the Gaussian PDF, it can achieve the emphasis along its original orientation and the diffused values over other orientations. From this viewpoint, there are several possibilities of computing the curvature.

- Gaussian PDF: This one has been discussed in the previous section. The Gaussian PDF has the biological support and it seems to perform well as mentioned in [7].
- $1/(K\cos\psi+\varepsilon)$ for the change of orientation ψ within [$-\pi/2$, $\pi/2$] and 0 elsewhere, where *K* is the controlling parameter and a tiny positive number ε is to avoid the division by 0. We originally thought this formula as an alternative to the Gaussian PDF. It can give an explicit relation between the curvature and the change of orientation and it does not allow the change of orientation for more than $\pi/2$, which seems reasonable to make the curve more smooth.
- $\exp(-K\cos\psi+\varepsilon)$ for the change of orientation ψ: This one is similar to the Gaussian PDF but it gives a clear indication on how the curvature changes as the result of the change in orientation.

We can even list more formulae for curvature computation. It seems to us that it is hard to judge which one is the best due to the fact of the lack of curve information. A better way for the curvature computation might be through iterations, i.e., in the first iteration, one could use any of the above formulae for the curvature computation and find out the most probable curve (This is under the assumption of no initial curvature information). After that, one could use the result from the first iteration to estimate the curvature and use it in the second iteration. Through each iteration, the curve information might become more and more accurate and it could help to do the shape completion better and better. Unfortunately, due to the limited time, we have not come up with a good scheme on how to do this. This could be our future work.

4.2 General calculation of transition probability

The calculation of the transition probability based on the general energy from Equation (12) is also an open question. One simple method to compute the transition probability is

$$P_{i,j}(\psi)=\exp\left(-E_{i,j}(\psi)\right) \qquad (13)$$

transformed from the energy $E_{i,j}(\psi)$ for the transition from the source pixel *i* to its neighboring pixel *j* with the angle ψ for the change in orientation. Since the equation (13) for the transition probabilities does not guarantee that the sum over all the possible transitions is 1, the normalization has to be done to achieve the final transition probabilities, i.e.,

$$\widetilde{P}_{i,j}(\psi) = P_{i,j}(\psi) / \sum_{\psi} P_{i,j}(\psi) \qquad (14)$$

It should be pointed out that the above computation is an intuitive approach to label each orientation with one probability: the labeling probability must reflect the curve energy. Of course, a traditional and formal approach is always to integrate all the possibilities within the quantized orientation interval as done in equation (4), and this might be useful if an iterative method can be done to improve the curvature estimate.

From the discussion in this section, we try to point out that the calculation of the transition probabilities developed in Section 3.2 is not unique and many other methods can be used. Due to the lack of the priori curve information, it is vague to say which method is the best for the completion fields. One possible way to improve the performance might be to estimate the curve information iteratively and use the estimated information for the calculation of the transition probabilities.

5 Illustrative Results

In this section, several results are presented to illustrate the stochastic completion field with probabilistic transition.

5.1 Validation of probabilistic transition

We first verify the use of probabilistic transition to characterize the behavior of the random walks. For this, we compare the approaches, namely, Monte Carlo simulation of random walks (SIM), theoretical calculation through the local current update equation (6) (THEO-1), and theoretical calculation through the overall transition matrix from equation (11) (THEO-2). We simulate 1×10^4 random walks with orientation at angle =0 radians. The other parameters considered are as follows.

- The variance σ^2 =0.25. The decay constant is set with τ =10. The number of orientations m =8. The number of steps (updates) N=20. The step-size of the random walk is set to 1 as a general parameter for which φ_0 and φ_1 from equation (3) are different.
- The relative probabilities are estimated by the fraction of $P(u,v)$ in each pixel to the largest number of $P(u,v)$ over all the pixels in the image, where $P(u,v)$ is the summation of $P(u,v,\phi)$ over all the orientations.

The results for the relative probabilities are tabulated in Table 1 in a 3×3 image with source in the state (2,2,0).

Table 1 Relative probabilities of each pixel in a 3×3 image with source in state (2,2,0)

Schemes	*row y \ column x*	*x=1*	*x=2*	*x=3*
SIM	*y=1*	*5e-4*	*1.65e-2*	*1.24e-1*
	y=2	*0*	*1.00*	*6.40e-1*
	y=3	*2e-4*	*1.85e-2*	*1.26e-1*
THEO-1	*y=1*	*4e-4*	*1.66e-2*	*1.28e-1*
	y=2	*1e-4*	*1.00*	*6.38e-1*
	y=3	*4e-4*	*1.66e-2*	*1.28e-1*
THEO-2	*y=1*	*4e-4*	*1.66e-2*	*1.28e-1*
	y=2	*1e-4*	*1.00*	*6.38e-1*
	y=3	*4e-4*	*1.66e-2*	*1.28e-1*

From the above table, we can see that

- The THEO-1 and THEO-2 are the same. This indicates that our implementation of the local concurrent update and that of the transition matrix are correct.
- Both THEO-1 and THEO-2 agree (approximately as only 10^4 random walks were simulated) with the corresponding results from SIM. This validates our theoretical analysis.
- From the intuitive perception, the relative probabilities in a 3×3 image with source point in the middle shall be symmetric with respect to the line of y=2. This symmetric property can be found very well achieved in the theoretical result but not in the simulation (SIM) from 10^4 random walks. To obtain more accurate results, huge number of random walks shall be simulated which of course is hard to reach due to the computer limitation.

We have conducted the similar simulation in the images with different sizes (4×4 and 8×8). As a check, the results in a 4×4 image with source in state (2,2,0) are listed in Table 2 for SIM and THEO-1 only as THEO-2 is the same as THEO-1. The results shown are supporting our previous statement: the analytical results from the local concurrent update agree well with the simulation results and they appear to be more accurate

Table 2 Relative probabilities of each pixel in a 4×4 image with source in state (2,2,0)

Schemes	*row y \ column x*	*x=1*	*x=2*	*x=3*	*x=4*
SIM	*y=1*	*6e-4*	*1.53e-2*	*1.32e-1*	*1.11e-1*
	y=2	*0*	*1.00*	*6.26e-1*	*4.07e-1*
	y=3	*7e-4*	*1.66e-2*	*1.36e-1*	*1.14e-1*
	y=4	*2.6e-3*	*1.21e-2*	*4.33e-2*	*6.75e-2*
THEO-1	*y=1*	*5e-4*	*1.66e-2*	*1.28e-1*	*1.14e-1*
	y=2	*2e-4*	*1.00*	*6.38e-1*	*4.09e-1*
	y=3	*7e-4*	*1.66e-2*	*1.28e-1*	*1.14e-1*
	y=4	*3.4e-3*	*1.34e-2*	*4.17e-2*	*6.99e-2*

than the simulation ones. Therefore, in the following, we will use THEO-1 to evaluate the stochastic completion fields. The reason that we choose THEO-1 instead of THEO-2 is due to the fact that for large-size images, THEO-1 appears to be simpler and easier to implement.

5.2 Effect of variance σ^2

In the following, we study the effect of the Gaussian variance σ^2. We still consider r=1, τ =10, m=8, and N=20. The results of $P(u,v,\phi)$ for σ^2=0.25 and σ^2=0.1 are plotted in Figure 5 and Figure 6, respectively.

To plot the relative probabilities with orientation, we use the following formula to compute the length l for the line (The arrow length is set relatively shorter than the line length).

$$l = \left[1 + s_f \cdot \log\left(P(u,v,\phi)\right)\right] \cdot L \qquad (15)$$

where s_f is the scaling factor set to 0.2 in the plot, L is the nominal length set to 0.8.

Note that the line length is automatically set to 0 whenever $l<0$ from the computation in equation (15) and only the pixels with $P(u,v,\phi)>10^{-9}$ will be plotted.

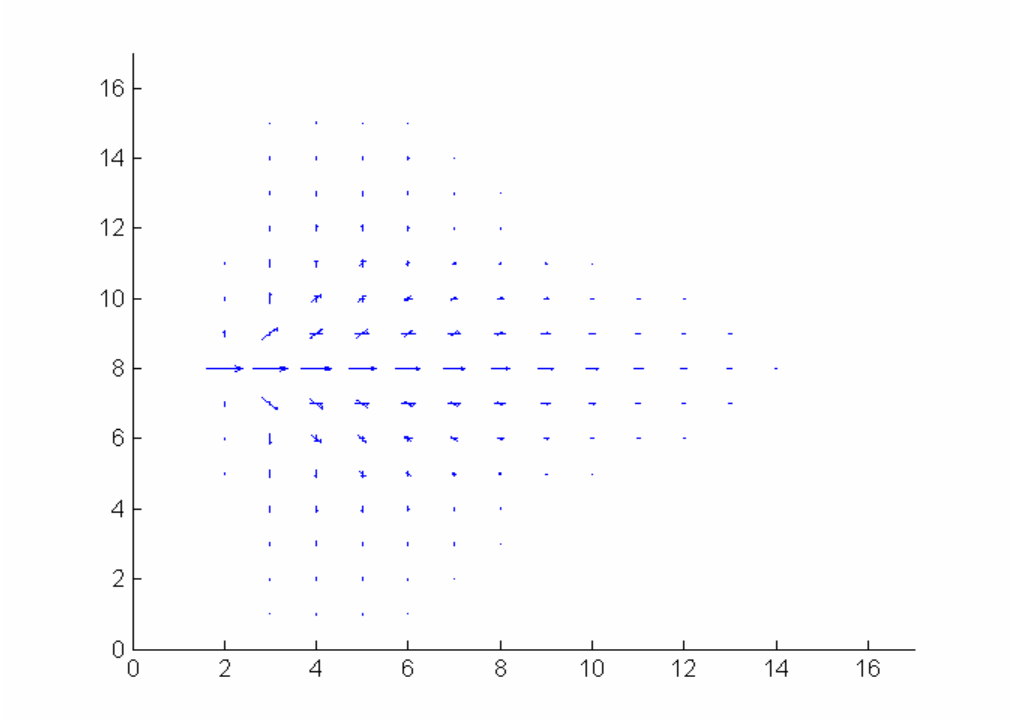

Figure 5 $P(u,v,\phi)$ in a 16×16 image with initial state (2,8,0) and r=1, τ =10, m=8, N=20, σ^2 =0.25.

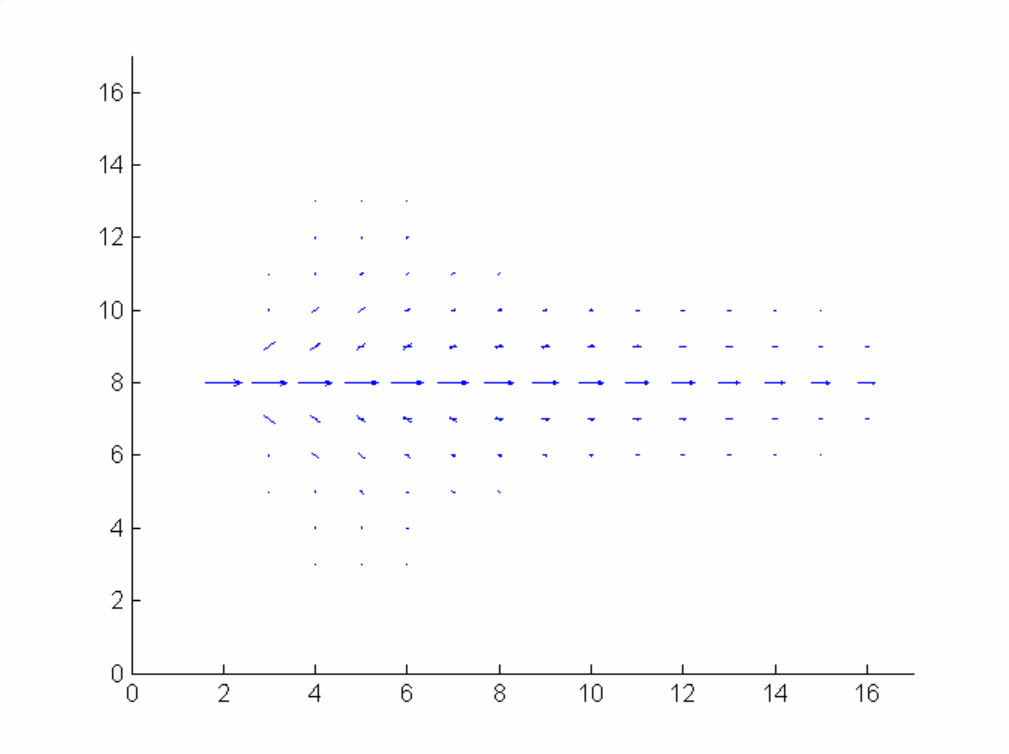

Figure 6 $P(u,v,\phi)$ in a 16×16 image with initial state (2,8,0) and *r*=1, τ =10, *m*=8, *N*=20, σ^2 =0.1

It can be seen from Figure 5 and Figure 6 that with larger σ^2 (=0.25), the probabilities over the pixels appear more spread out, while with smaller σ^2, the probabilities are more restricted along with the original orientation.

5.3 Effect of decay constant

The effect of decay constant is studied next. We consider *r*=1, *m*=8, N=20, and σ^2 =0.25. The results of $P(u,v,\phi)$ for τ =1 are plotted in Figure 7.

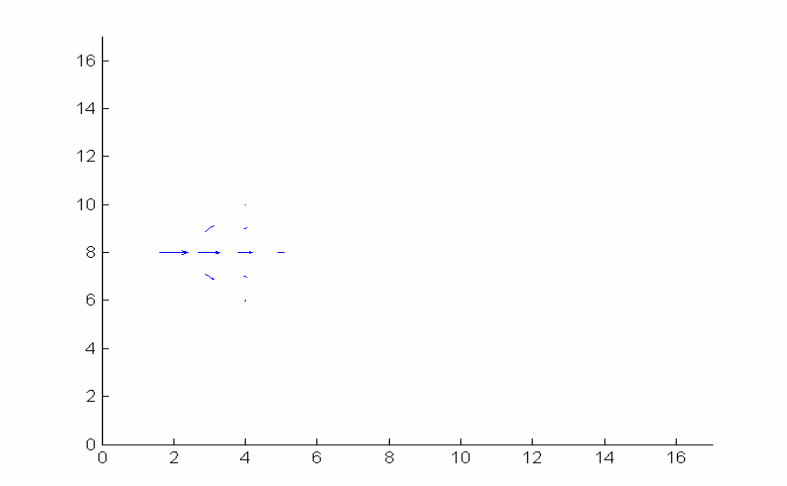

Figure 7 $P(u,v,\phi)$ in a 16×16 image with initial state (2,8,0) and *r*=1, τ =1, *N*=20, σ^2 =0.25

Comparing Figure 7 for τ =1 with Figure 5 for τ =10, we can see that with smaller τ in Figure 7, the random walks have a shorter lifetime so the corresponding probabilities in the pixels plotted in the figure die out very faster.

5.4 Examples of completion fields

We present several results for the completion fields by using the local current approach in Section 3.2.2. According to equation (5), we set the step-size *r* to 1/2sin(π/8)=1.31 that is the best choice in terms of fairness for all the possible orientations. So far, we have considered the number of orientations *m*=8, which is very simple in evaluating the effect of various parameters. For the completion fields below, however, *m*=8 appears to be not good enough due to the fact that with *m*=8, the orientation begins at the source point can be easily changed by $\pi/4$ in one step and in most cases the change of orientation will point to the sink point and thus the straight line seems to be the choice to complete the shape between the source and sink points. We have observed this from our simulation results (not shown for the sake of brevity). To improve the quality of shape completion, we have no choice but to consider more orientations.

In all the following simulations, we consider the number of orientations *m*=16. Further, to present well the results, after the computation of the stochastic source and sink fields, we further group nine pixels as one. This is like a second-level of quantization on pixels with interval =3. After the quantization, we compute the stochastic completion field $C(u,v,\phi)$ according to equation (9) (We tried to do the computation before the quantization and the results appeared not good).

Next, we consider the case of four source/sink points around the circumference of a circle at the state (x,y,θ)=(3,16,8), (16,29,12), (29,16,0), (16,3,4). Its stochastic source, sink, and completion fields are shown in Figure 8, Figure 9, and Figure 10, respectively, where the probabilities of nine neighboring pixels are grouped as one (This is like the second-level of quantization on both *x* and *y* axes). Please note that due to the second level of quantization, the original four points might not be shown explicitly but their neighboring pixels are. The plot is following the logarithm mapping in equation (15) but with *L*=2.4. The probability thresholds for plotting are 1E-4 in Figure 8 and Figure 9, and 1E-5 in Figure 10.

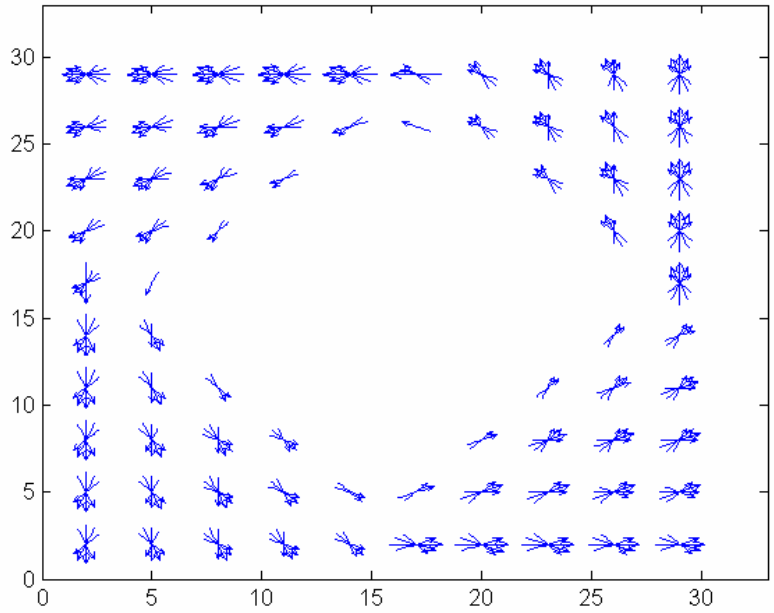

Figure 8 Stochastic source field in a 32 × 32 image with *r*=1.31, τ =10, *m*=16, *N*=32, σ^2 =0.01.

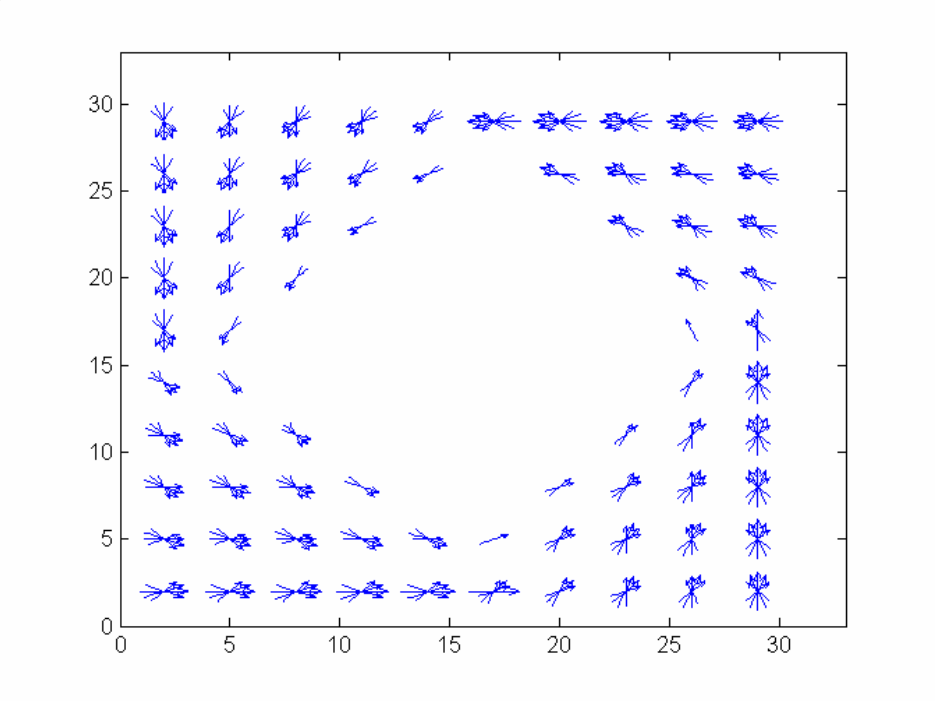

Figure 9 Stochastic sink field in a 32×32 image with r=1.31, τ =10, m=16, N=32, σ^2 =0.01.

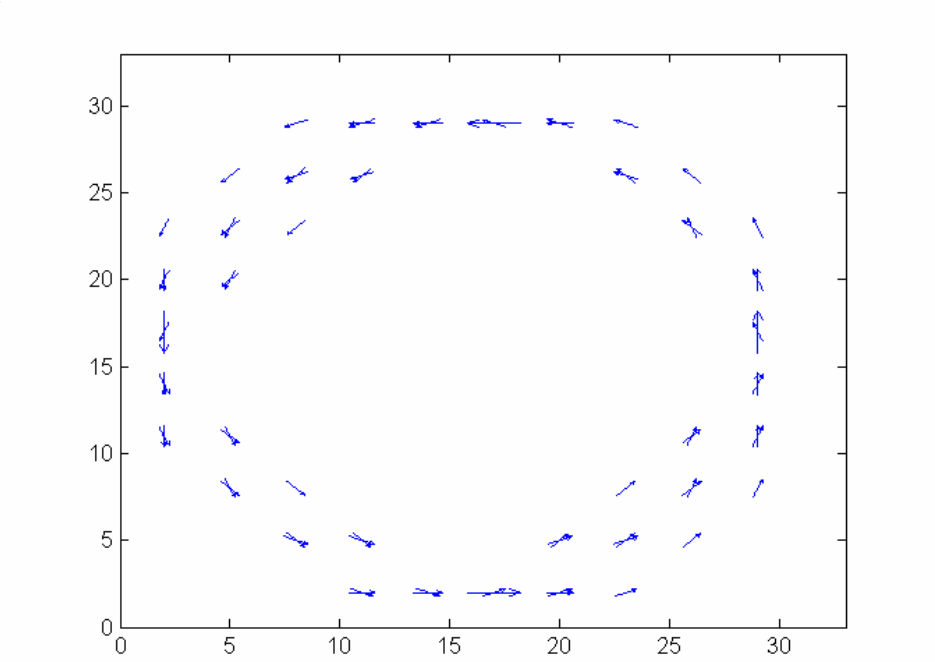

Figure 10 Stochastic completion field in a 32×32 image with r=1.31, τ =10, m=16, N=32, σ^2 =0.01.

The results shown in Figure 8, Figure 9, and Figure 10 are found similar to the corresponding figures in [7] and they demonstrate the good performance of the simplified approach from equation (6) for the stochastic completion field.

We have to point out that as mentioned in Section 4, several other formulae can be used to compute the energy related to distance and curvature and they might result in different transition probabilities for the

stochastic completion field. At the current level of simulation in terms of no initial curvature information and tuning parameters to achieve good results, it seems that those formulae can present the similar results as the ones shown in this section. Therefore, we will not repeat the results here. In the following, we still use the main approach presented in Section 3 for simulation.

Other examples for the source/sink pairs: (2,23,2)/(46,23,12) and (2,23,2)/(46,23,2) are carried out and the stochastic completion fields shown in Figure 11-Figure 12, and Figure 13-Figure 14, respectively. To show the results nicely, the probability thresholds used for plotting are 7E-6, 1E-5, 5E-6, and 1E-5 in Figure 11, Figure 12, Figure 13, and Figure 14, respectively. Again, due to the second-level quantization the source/sink positions are not explicitly shown in those four figures. However, their effect for the stochastic completion field is clear. Note that for the second source/sink pair, we need to diffuse the random walk more and the variance σ^2 is set to 0.05 in Figure 13 and Figure 14 as compared with σ^2=0.02 for the first source/sink pair in Figure 11 and Figure 12. Overall, with the simple probabilistic approach, the stochastic completion field can be easily computed and the resulting performance appears acceptable especially in the plot with orientation in Figure 11 and Figure 13. Compared with the corresponding figures in [7], our plots with intensity in Figure 12 and Figure 14 seem not good enough due to the low resolution as we considered 48×48 image only. Currently, the image size in our implementation based on the Matlab platform is limited by the hardware in terms of memory and speed. However, we believe that if we consider high resolution with more pixels, our intensity plots will become better.

As a summary, the illustrative results presented in this section demonstrate the use of the simplified approach based on the probabilistic transition for the stochastic completion field. The computation is simple and the results appear to be acceptable.

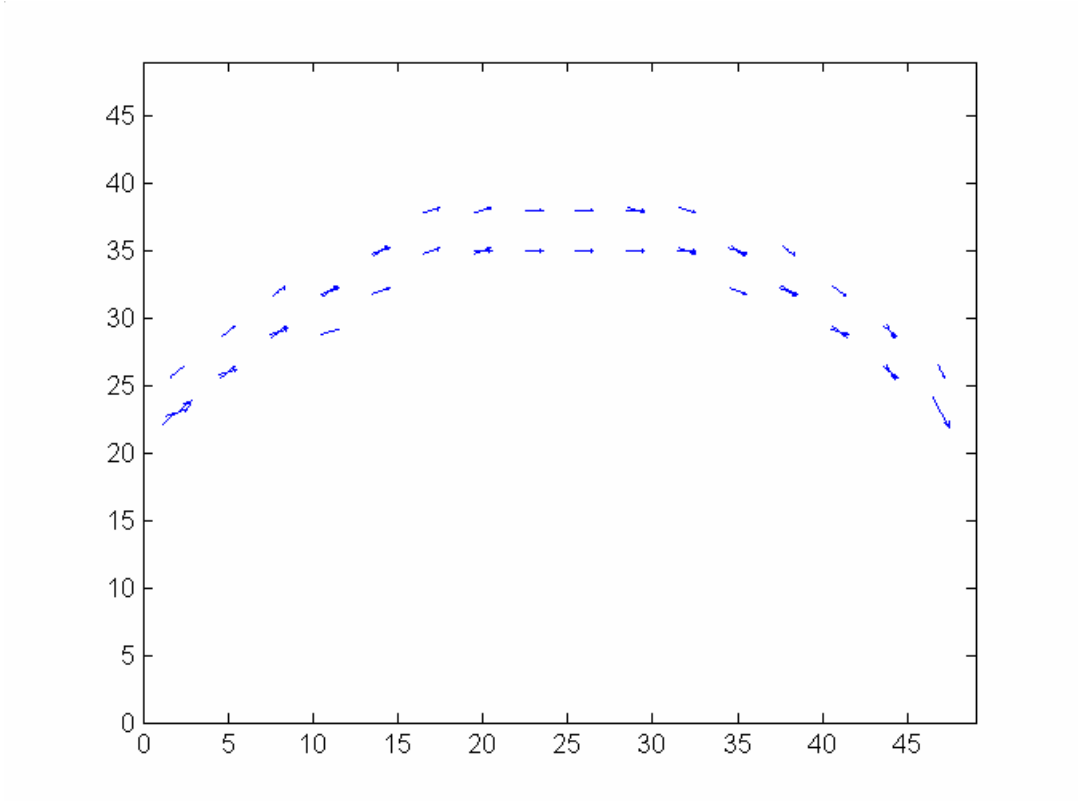

Figure 11 Stochastic completion field with orientation for source/sink pair: (2,23,2)/(46,23,12), in a 48 × 48 image with *r*=1.31, τ =10, *m*=16, *N*=48, σ^2 =0.02.

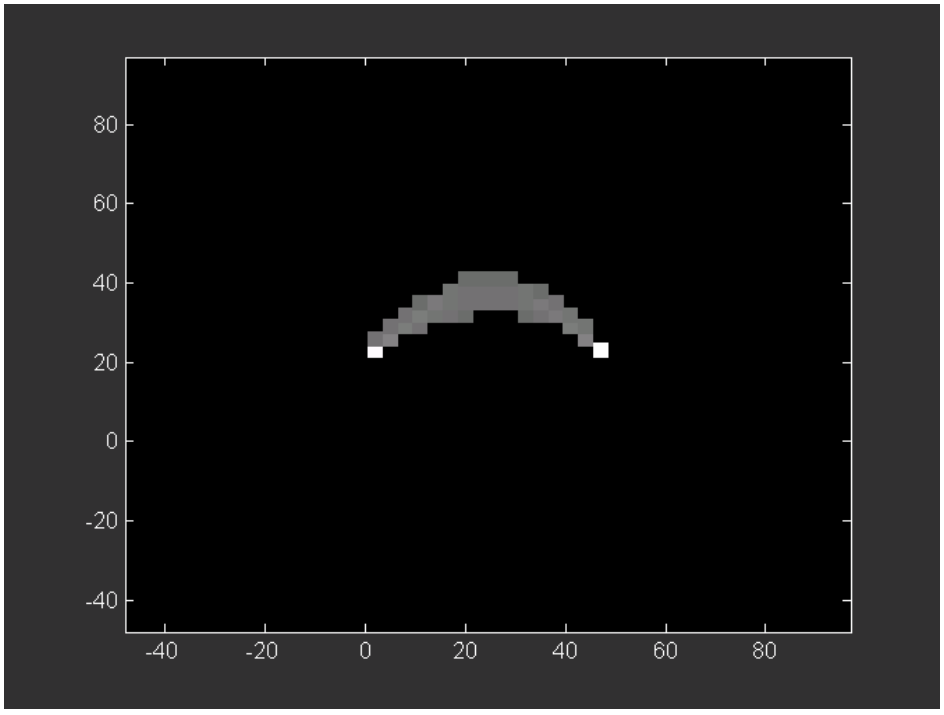

Figure 12 Stochastic completion field with intensity for source/sink pair: (2,23,2), (46,23,12), in a 48 × 48 image with *r*=1.31, τ =10, *m*=16, *N*=48, σ^2 =0.02.

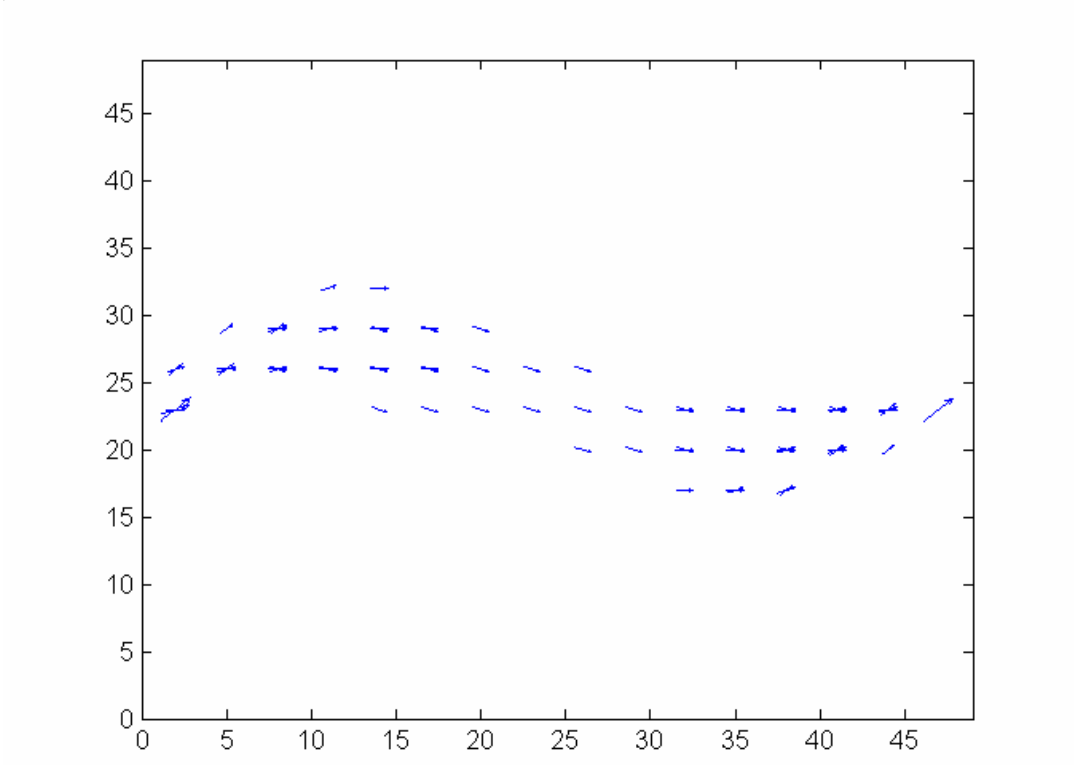

Figure 13 Stochastic completion field with orientation for source/sink pair: (2,23,2)/(46,23,2), in a 48 × 48 image with *r*=1.31, τ =10, *m*=16, *N*=48, σ^2 =0.05.

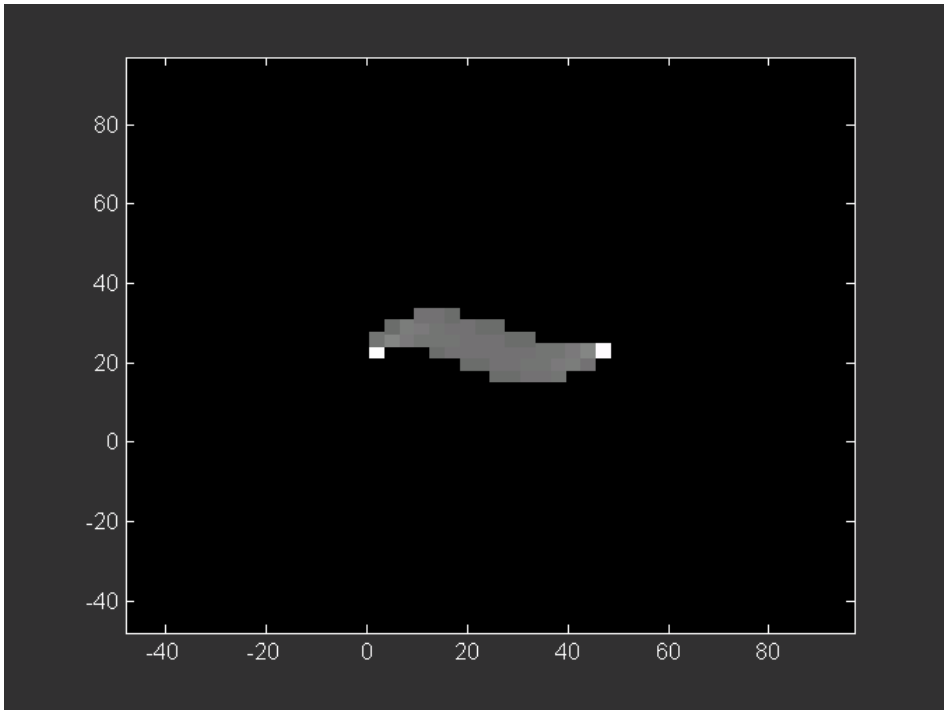

Figure 14 Stochastic completion field with intensity for source/sink pair: (2,23,2)/(46,23,12), in a 48 × 48 image with *r*=1.31, τ =10, *m*=16, *N*=48, σ^2 =0.05.

6 Conclusions and Future Work

In this report, we have discussed the use of transition probabilities for stochastic completion field. It has been shown that by considering the actual line-up of the image pixels and the quantization for the random walk position, the stochastic completion field can be well characterized by the transition probabilities from its current pixel to its eight neighboring pixels. Those transition probabilities are the same for all the pixels in the image, they can be pre-computed, and they render the computation be carried out in a parallel (concurrent) fashion. The stability consideration and the steady state solution are discussed and it is shown that the stability of the stochastic completion field with probabilistic transition is assured by selecting a good decay factor and the steady state solution can be computed directly from the transition matrix. Unfortunately, the computation of the steady state solution involves a matrix inverse with a size of $n^2m \times n^2m$ for $n \times n$ image and m orientations (In our case, m=8 or 16). Therefore, for large size image, a local current update equation has to be used to analytically compute the relative probabilities of the pixels in the image. The resulting computational complexity is O(nmt) for t updates, which is inline with the local parallel computation in [9]. However, unlike the one in [9], which used an approximation for the integral estimate, the local computation approach presented in this report is the natural one resulted from the line-up of the image pixels and quantization assumptions and it does not need an approximation for the integral. Some discussions on the general computation of the curvature energy and the transition probabilities are also carried out. It appears to us that the Gaussian PDF is a good selection but it is not a unique one and there are other choices. Finally, several illustrative results are presented to compare our approach with the one from the simulation in [7] and check the effects of variance and decay factor. It is shown that the analytical results from the stochastic completion field with probabilistic transition are in good agreement with those from the Monte Carlo simulation of random walks and they can provide a good performance in solving the completion shape and salience problem.

As we can see from this report, there are still some unanswered questions and interesting research areas in the completion field that need contribution from researchers. Several examples are

- Determine the proper values for parameters σ^2, τ: The choices of those parameters could determine the diffusion process and affect the performance of the completion fields. Right now, their choices are based on the intuitive guess and the final results appearance.
- Study the effect of step-size r: In this report, we considered only the smallest step-size (under quantization) to have a fine-tuning in the curve estimate. To reduce further the complexity and compute the stochastic completion field quickly, it is of interest to see the effect of varying step-size r, the increase of which may introduce more neighboring pixels for the possible next-step positions.
- Explore the best choice for the computation of the curvature and transition probabilities: This is a rather important and very interesting work. One possible approach as mentioned in Section 4 is to compute the completion field iteratively. From one iteration to another, one can estimate curvature information and use it as a guideline instead of the Gaussian PDF. It is expected that this iterative approach could lead to a better solution to the completion fields.
- How to quantitatively judge the performance of the stochastic completion field? Right now, there seems missing quantitative measure to judge the performance of the stochastic completion field. Although the freedom from any explicit minimization is considered to be a positive point for the stochastic completion field, it seems difficult to say which approach is the best without the explicit quantitative criterion.

We believe that with dedication and hard-work, further research and development in the area of shape analysis could lead good techniques to solve with satisfaction the completion shape and salience problem and they can be very much useful in computer vision and image processing.

7 Acknowledgments

We are grateful to the instructor Prof. Kaleem Siddiqi for presenting us very interesting lectures in the area of shape analysis and help us with good reference papers and constructive suggestions in our project. We also like to acknowledge with pleasure the support and effort from the students who took this course COMP766 and created a good environment for learning.

8 References

[1] Marr, D., *Vision*, W. H. Freeman and Company, New York, 1982.

[2] Ullman, S. "Filling-in the gaps: the shape of subjective contours and a model for their generation", Biological Cybernetics, no.21, pp.1-6, 1976.

[3] Grossberg, S. and Mingolla, E., "Neural dynamics of form perception: boundary completion, and illusory figures, and neon color spreading", Psychological review, 92, pp.173-211, 1985.

[4] Parent, P. and Zucker, S. W., "Trace inference, curvature consistency and curve detection", IEEE Trans. Pattern analysis and machine intelligence, 11, pp.823-889, 1989.

[5] David, C. and Zucker, S. W., "Potentials, valleys, and dynamic global covering", Int. J. Computer Vision, vol.5, no.3, pp.219-238, 1990.

[6] Guy, G. and Medioni, G., "Inferring global perceptual contours from local features", Proc. of DARPA Image Understanding Workshop, Washington, D. C., pp.881-892, 1993.

[7] Williams, L. R. and Jacobs, D. W., "Stochastic completion fields: a neural model of illusory contour shape and salience", Proc. 5th Int. Conf. Computer Vision, Cambridge, Mass., 1995.

[8] Thornber, K. K. and Williams, L. R., "Analytic solution of stochastic completion fields", Biological Cybernetics 75, pp.141-151, 1996.

[9] Williams, L. R. and Jacobs, D. W., "Local parallel computation of stochastic completion fields", Neural Computation, 9(4), May 1997.

[10] Mumford, D., *Elastica and Computer vision, algebraic geometry and its applications*, Springer-Verlag, New York, 1994.

[11] Hubel, D. H. and Wiesel, T. N., "Receptive fields, binocular interaction and functional architecture in the cat's visual cortex". J. Physiol., Lond., 160, pp.106-154. 1962.

[12] Hubel, D. H. and Wiesel, T. N., *Brain mechanisms of vision*, Scientific American, vol. 241, pp. 150-162, Sept. 1979.

[13] Blasdel, G. and Obermeyer, K., "Putative strategies of scene segmentation in monkey visual cortex", Neural Networks, vol.7, no.6/7, pp.865-881, 1994.